Title

Prospective comparison of longitudinal change in hepatic proton density fat fraction (PDFF) estimated by magnitude-based MRI (MRI-M) and complex-based MRI (MRI-C)

Journal

European Radiology, 30(9)

ISSN

0938-7994

Authors

Mamidipalli, Adrija
Fowler, Kathryn J
Hamilton, Gavin
et al.

Publication Date

2020-09-01

DOI

10.1007/s00330-020-06858-x

Peer reviewed

Published in final edited form as:

Eur Radiol. 2020 September ; 30(9): 5120–5129. doi:10.1007/s00330-020-06858-x.

Prospective comparison of longitudinal change in hepatic proton density fat fraction (PDFF) estimated by magnitude-based MRI (MRI-M) and complex-based MRI (MRI-C)

Adrija Mamidipalli[1], **Kathryn J. Fowler**[1], **Gavin Hamilton**[1], **Tanya Wolfson**[2], **Yesenia Covarrubias**[1], **Calvin Tran**[1], **Soudabeh Fazeli**[1], **Curtis N. Wiens**[3], **Alan McMillan**[3], **Nathan S.**

Adrija Mamidipalli adrijamamidipalli@gmail.com, Claude B. Sirlin csirlin1@gmail.com.

Electronic supplementary material The online version of this article (https://doi.org/10.1007/s00330-020-06858-x) contains supplementary material, which is available to authorized users.

Guarantor The scientific guarantor of this publication is Dr. Claude B. Sirlin.

Conflict of interest The authors of this manuscript declare relationships with the following companies: Effort by Dr. Luke M. Funk on this study was made possible by a VA Career Development Award (CDA 015–060). The views presented are those of the authors and not those of the DVA or the US Government. There are no relevant conflicts of interest or industry support.

Disclosure statement Dr. Sirlin consults and advises for Alexion, AstraZeneca, Bioclinica, BMS, Fibrogen, Galmed, Genzyme, Gilead, Icon, Intercept, Isis, Janssen, NuSirt, Perspectum, Pfizer, Profil, Sanofi, Shire, Synageva, Tobira, Takeda, and Virtualscopics. He received grants from Siemens, GE, and Guerbet.
Dr. Middleton consults for Kowa, Median, and Novo Nordisk, and has been involved in university service contracts with Alexion, AstraZeneca, Bristol-Myers Squibb, Enanta, Gilead, Guerbet, Intercept, Pfizer, Roche, Shire, and Synageva.
Dr. Reeder consults for ArTara Therapeutics, and has ownership interests in Calimetrix, Reveal Pharmaceuticals, Cellectar Biosciences, and Elucent Medical. The University of Wisconsin receives research support from GE Healthcare and Bracco Diagnostics.
Dr. Schwimmer consults for Novo Nordisk, and has received grant support from Galmed and Intercept.
All other authors report no conflict of interest, and no relationships with any companies, whose products or services may be related to the subject matter of the article.
Each of my co-authors and I have made substantial contributions to all phases of manuscript development. We have all approved the final version prior to submission.
Statistics and biometry Dr. Anthony Gamst and Tanya Wolfson kindly provided statistical advice for this manuscript, and were included as authors, and kindly provided statistical advice for this manuscript.
Informed consent Written informed consent was obtained from all subjects (patients) in this study.
Ethical approval Institutional Review Board approval was obtained.

Study subjects or cohorts overlap Some study subjects or cohorts have been previously reported in:
We have previously published two papers (PDFs attached) based on data from the parent weight loss surgery (WLS) program, with different aims from our current aims. Those papers were:
1. Fazeli Dehkordy S, Fowler KJ, Mamidipalli A, et al Hepatic steatosis and reduction in steatosis following bariatric weight loss surgery differs between segments and lobes. Eur Radiol. 2018; 13. https://doi.org/10.1007/s00330–018-5894–0 [PMID: 30547206] [Epub ahead of print] [reference #24 in this paper; details redacted in the references section]
This paper looked at segmental PDFF (proton density fat fraction) values estimated by (only) MRI-M in 118 adults undergoing bariatric surgery. The aims were to evaluate PDFF distribution estimated using MRI-M across liver segments at baseline and compare longitudinal segmental PDFF changes across time points.
2. Pooler BD, Wiens CN, McMillan A, et al Monitoring fatty liver disease with MRI following bariatric surgery: a prospective, dual-center study. Radiology. 2018; 290:682–69018 [Epub ahead of print] [PMID: 30561273] [reference #25 in this paper; details redacted in the references section]
This paper looked at whole-liver PDFF values estimated using (only) MRI-C in 50 adults undergoing bariatric surgery. The aims were to longitudinally monitor PDFF estimated using MRI-C, taking into account possible effects of changes in BMI, weight, and waist circumference.
This current analysis included 54 adults from the parent WLS who had whole-liver PDFF □ 5% estimated by both MRI-M and MRI-C, and compared the rate of change of PDFF with these two MRI techniques (MRI-M and MRI-C), which was not reported in the two prior papers.
Methodology
Retrospective
Observational
Multi-center study

Artz[3], **Luke M. Funk**[4,5], **Guilherme M. Campos**[4], **Jacob A. Greenberg**[4], **Anthony Gamst**[2], **Michael S. Middleton**[1], **Jeffrey B. Schwimmer**[6,7], **Scott B. Reeder**[8], **Claude B. Sirlin**[1]

[1]Liver Imaging Group, Department of Radiology, University of California - San Diego, San Diego, CA, USA

[2]Computational and Applied Statistics Laboratory, Supercomputer Center, University of California - San Diego, San Diego, CA, USA

[3]Department of Radiology, University of Wisconsin, Madison, WI, USA

[4]Department of Surgery, University of Wisconsin, Madison, WI, USA

[5]William S. Middleton VA, Madison, WI, USA

[6]Division of Gastroenterology; Hepatology and Nutrition; Department of Pediatrics, University of California, San Diego, La Jolla, CA, USA

[7]Department of Gastroenterology, Rady Children's Hospital, San Diego, CA, USA

[8]Departments of Radiology, Medical Physics, Biomedical Engineering, Medicine, and Emergency Medicine, University of Wisconsin, Madison, WI, USA

Abstract

Purpose—To compare longitudinal hepatic proton density fat fraction (PDFF) changes estimated by magnitude- vs. complex-based chemical-shift-encoded MRI during a weight loss surgery (WLS) program in severely obese adults with biopsy-proven nonalcoholic fatty liver disease (NAFLD).

Methods—This was a secondary analysis of a prospective dual-center longitudinal study of 54 adults (44 women; mean age 52 years; range 27–70 years) with obesity, biopsy-proven NAFLD, and baseline PDFF ≥ 5%, enrolled in a WLS program. PDFF was estimated by confounder-corrected chemical-shift-encoded MRI using magnitude (MRI-M)- and complex (MRI-C)-based techniques at baseline (visit 1), after a 2- to 4-week very low–calorie diet (visit 2), and at 1, 3, and 6 months (visits 3 to 5) after surgery. At each visit, PDFF values estimated by MRI-M and MRI-C were compared by a paired *t* test. Rates of PDFF change estimated by MRI-M and MRI-C for visits 1 to 3, and for visits 3 to 5 were assessed by Bland-Altman analysis and intraclass correlation coefficients (ICCs).

Results—MRI-M PDFF estimates were lower by 0.5–0.7% compared with those of MRI-C at all visits ($p < 0.001$). There was high agreement and no difference between PDFF change rates estimated by MRI-M vs. MRI-C for visits 1 to 3 (ICC 0.983, 95% CI 0.971, 0.99; bias = − 0.13%, $p = 0.22$), or visits 3 to 5 (ICC 0.956, 95% CI 0.919–0.977%; bias = 0.03%, $p = 0.36$).

Conclusion—Although MRI-M underestimates PDFF compared with MRI-C cross-sectionally, this bias is consistent and MRI-M and MRI-C agree in estimating the rate of hepatic PDFF change longitudinally.

Keywords

Nonalcoholic fatty liver disease; Magnetic resonance imaging; Longitudinal study

Introduction

Accurate MRI-based quantitative techniques for estimating liver fat have been developed. Proton density fat fraction (PDFF), which is the proportion of mobile protons attributable to tissue triglyceride, can be estimated using confounder-corrected chemical-shift-encoded MRI (CSE-MRI) [1–3]. There are two general techniques for acquiring PDFF, broadly classified as magnitude-based MRI (MRI-M) and complex-based MRI (MRI-C) [1–8]. MRI-M uses only magnitude data and, if signal from water is dominant, can estimate PDFF from ~ 0–50%, whereas MRI-C uses both phase and magnitude data and can estimate PDFF from ~ 0–100%. While a dynamic range of 0–100% is important for imaging adipose tissue, it may not be necessary of hepatic PDFF, which infrequently exceeds 50% [1]. Both techniques use low flip angle to minimize T1 weighting effects, acquire multiple echoes to allow for T2* correction and separate fat and water signals, and incorporate a multi-peak spectral model to account for the spectral complexity of fat [1, 3]. Numerous studies have shown that MRI-M and MRI-C accurately quantify hepatic PDFF despite the modeling and technical parameter differences between them [1, 8–11].

As a noninvasive quantitative imaging biomarker of hepatic steatosis, PDFF has been validated against histology and biochemically determined triglyceride concentration in animal studies [12, 13], human liver tissue [14–18], and both pediatric and adult clinical patients [18, 19]. Due to its high precision and accuracy, PDFF is being used increasingly by radiology practices worldwide for clinical care of patients with nonalcoholic fatty liver disease (NAFLD) [20–22], the most common chronic liver disease in children and adults [23], and it has been applied as an endpoint in multiple clinical trials [20, 21, 24, 25]. Studies have shown that both MRI-M and MRIC accurately estimate hepatic PDFF in cross-sectional analyses when compared with reference standards of magnetic resonance spectroscopy (MRS) [4, 8–11] and histology [14–18]. However, MRI-M PDFF estimations are on average ~ 0.6% lower than those from MRI-C [11, 26], which may introduce errors in the assessment of longitudinal change if the techniques are used interchangeably in the same patient.

Due to concerns about assessment of longitudinal change, most industry and federally funded prospective multi-center NASH clinical trial sponsors currently mandate that either MRI-M or MRI-C, but not both, be used study-wide. The mandate to use only one technique may exclude some otherwise qualified centers to participate if they do not have access to the mandated option. The decision to mandate a single technique in clinical trials may be unnecessary. The bias between MRI-M and MRI-C is small and if consistent, it is likely that the two techniques would agree in estimating PDFF change longitudinally. Demonstration that the two techniques agree in estimating longitudinal PDFF change would allow sites to select the technique that is available to them for participation in clinical trials, thus increasing the flexibility for site qualification and participation. Additionally, as more and more radiology practices are called upon to produce quantitative liver fat results, radiologists will need to be aware of PDFF measurement options and their implications for measuring longitudinal changes in patients.

The purpose of this study was to determine if the bias between these two techniques of PDFF estimation would be constant across longitudinal changes, allowing for similar estimations of PDFF change over time. If constant, this would imply that either technique could be used for longitudinal assessment of change in clinical care and in clinical trials.

Methods

Research participants and study design

This was a secondary, longitudinal analysis of MRI-PDFF data collected as part of a prospective bi-center study of dietary and surgical intervention for obesity class II [27] or higher, performed at two academic weight loss surgery (WLS) centers. Both centers had similar WLS programs consisting of 2–4 weeks of a very low–calorie diet (VLCD, 0.6–0.9 kcal/day) followed by bariatric surgery.

This secondary analysis and the parent study were approved by an Investigational Review Board and are compliant with the Health Insurance Portability and Accountability Act and participants provided written informed consent.

For the parent study, participants with severe obesity were recruited consecutively from the two centers from June 2010 to December 2015. Inclusion criteria were BMI ≥ 35 kg/m^2, being considered for bariatric surgery (laparoscopic Roux-en-Y gastric bypass, or sleeve gastrectomy), and willingness to participate in all study procedures. Exclusion criteria were contraindications to MR imaging, history of liver disease other than NAFLD, or inability to fit in the magnet bore. Enrolled patients underwent up to five MRI exams [28, 29]. PDFF was estimated at baseline (visit 1), and immediately after completion of their VLCD (visit 2). For patients already started on the VLCD prior to study recruitment, visit 1 was omitted from the analysis and their first visit was labeled as visit 2, to be consistent with the overall cohort. Left-lobe intraoperative biopsies were performed during bariatric surgery. Patients with NAFLD confirmed by intraoperative biopsy (i.e., presence of at least grade 1 steatosis or higher on biopsy) were offered follow-up MRI at 1, 3, and 6 months after WLS (visits 3, 4, and 5, respectively). Demographic and clinical data were collected at baseline, and anthropometric information was collected at each visit for all participants.

For this secondary analysis, participants from the parent study were included if they had both MRI-M and MRI-C at 3 T on at least two visits and if baseline whole-liver PDFF was ≥ 5%.

Adults enrolled in a WLS program constitute an ideal cohort for comparing longitudinal change measurements by MRI-M and MRI-C, as the patients have a wide range of baseline PDFF values and reliable longitudinal reduction of PDFF. Importantly, PDFF reduction tends to be biphasic, with a rapid decrease in PDFF in the preoperative/ perioperative periods followed by a slower decrease in the postoperative period [28, 29]. This biphasic behavior allows comparison of both MRI techniques during different phases of PDFF reduction.

MRI exams

Participants were asked to fast for at least 4 h before each MRI exam to minimize potential confounding physiological effects. At one center, MRI was acquired on a 3 T MRI (GE Signa Twin-Speed EXCITE HDxt, 8-element torso phased array coil with dielectric pads placed over the abdomen to reduce B1 heterogeneity; GE Healthcare). At the other center, MRI was acquired on a 3 T MRI (GE 750, 32-element torso phased array coil without dielectric pads; GE Healthcare). For all examinations, phased array surface coils were centered over the liver and each MR exam lasted approximately 60 min. PDFF was estimated using MRIM and MRI-C at all visits. Both techniques used a flip angle that minimized T1 weighting for the acquisition repetition time [9, 30–32]. A rectangular field of view and coverage was adjusted to the patient's body habitus and breath-hold capacity. The MR parameters, summarized in Table 1, followed the guidelines set out by the Quantitative Imaging Biomarkers Alliance PDFF committee [30].

MRI analysis

A separate fitting algorithm was applied to the source images pixel-by-pixel by the MRI scanner system software to reconstruct parametric PDFF and R2* maps for each technique [29–32]. The MRI-M technique used a magnitude data algorithm and the MRI-C technique used a complex data algorithm. Both algorithms assumed exponential R2* signal decay [31–36] and applied the same multi-peak fat-spectral model derived from human liver triglyceride composition [37].

Source images and the PDFF and R2* parametric maps were transferred offline for analysis. Using OsiriX software version 7.0.3 (OsiriX Foundation), source images and PDFF maps were reviewed by trained image analysts (WH, JH ≥ 5 years of experience) blinded to all clinical and demographic data. A 1-cm radius circular region of interest (ROI) was manually placed in each of the nine Couinaud liver segments on the fifth-echo MRI-M source images, avoiding major vessels and bile ducts, liver edges, the gallbladder, any lesions, and artifact. The fifth-echo images were used because they consistently provided adequate anatomic delineation for ROI placement. ROIs were co-localized manually across time points to those placed for the baseline visit. At each time point, the nine ROIs were copied onto the MRI-C water images in a similar fashion to that described above, and manually adjusted as needed for co-localization. The nine ROIs were subsequently copied to the corresponding locations on the PDFF parametric maps for both techniques without additional adjustment. ROIs were placed and adjusted on anatomic images rather than PDFF maps to eliminate information bias. The mean PDFF value of each ROI was recorded at each time point for each technique.

Statistical analysis

All statistical analyses were performed by a staff statistician under the supervision of a faculty statistician (TW and AG, respectively, both with over 20 years of experience), using R version 3.5.1 (2018, GNU Public License, R Foundation for Statistical Computing). Cohort characteristics were summarized descriptively. For each technique and time point, the PDFF values from the nine ROIs were averaged to yield a single whole-liver PDFF value. At each visit, PDFF values estimated by MRI-M and MRI-C were compared by a paired *t* test.

As previously reported, PDFF reduction during a VLCD-bariatric surgery program tends to be biphasic, with rapid linear decline in the preoperative/perioperative periods (i.e., from visits 1 to 3) and slow linear decline in the postoperative period (i.e., from visits 3 to 5) [28, 29]. Accordingly, we used linear regression to calculate rates of hepatic PDFF change for each individual participant for separately for the preoperative/perioperative period (visits 1 to 3, $n = 54$ patients) and for the postoperative period (visits 3 to 5, $n = 40$ patients) (Fig. 1). Rates of change were expressed as changes in PDFF per month. The reason for estimating and analyzing rates of change (rather than analyzing first-last visit differences for each time period) was to ensure the use of all available patient information, including the middle visits. Additionally, rates of change are, by definition, standardized to the same time units for all patients, which ensures comparability given the variable lengths of per-patient time periods.

Agreement and differences between rates of PDFF change estimated by MRI-M and MRI-C were assessed by Bland-Altman analysis and intraclass correlation coefficients (ICCs) for visits 1–3, and for visits 3–5, separately. Baseline and final BMI were summarized descriptively. Relationships between baseline BMI, baseline PDFF, and rates of PDFF change were informally explored.

Results

Cohort characteristics are summarized in Table 2, and a flow chart of study cohort is shown in Fig. 1. A total of 44 women and 10 men (mean age 52 years; range 27 to 70) from the two study sites met inclusion criteria for this secondary analysis (i.e., patients with both MRI-M and MRI-C imaged at 3 T on at least two visits and baseline whole-liver PDFF ≥ 5%). All participants had a baseline visit (visit 2 served as baseline for two participants), and at least two visits in the visit 1 to 3 period. Forty participants had at least two visits during the visit 3 to 5 period. A total of 29 participants had all five visits.

Figure 2 presents PDFF over time for the two techniques, both as individual trajectories and visit averages. At each visit, MRI-M PDFF was lower by 0.5–0.7% than MRI-C PDFF ($p < 0.001$ at each visit). Per-visit PDFF summaries by the two techniques are presented in Table 3.

As estimated by MRI-M, PDFF decreased on average by 5.3% per month for visits 1 to 3, and 0.8% per month for visits 3 to 5 (Fig. 2). As estimated by MRIC, PDFF decreased by 5.2% per month for visits 1 to 3, and by 0.8% per month for visits 3 to 5. BMI decreased by 2.9 kg/m^2 per month for visits 1 to 3, and by 1.1 kg/m^2 per month for visits 3 to 5.

There was high agreement and no difference between PDFF change rates estimated by MRI-M and MRI-C for visits 1 to 3 (ICC 0.98, 95% CI 0.971–0.99; BA bias 0.13%; $p = 0.22$), or for visits 3 to 5 (ICC 0.96, 95% CI 0.92–0.98; BA bias 0.03%; $p = 0.36$) (Fig. 3; and supplementary Fig. 1). Figure 3a (visits 1 to 3) and b (visits 3 to 5) are color coded by baseline BMI; and supplementary Fig. 1a (visits 1 to 3) and 1b (visits 3 to 5) are color coded by baseline PDFF to illustrate their distribution pattern over time. Agreement for rate of PDFF change by both MRI techniques was unrelated to baseline BMI and PDFF for visits 1 to 3 and 3 to 5.

Figure 4 illustrates PDFF changes estimated by MRI-M and MRI-C, from visits 1 to 5 with both techniques in a 52-year-old woman.

Discussion

In this prospective two center study, we analyzed PDFF data from obese adults with biopsy-proven NAFLD who were enrolled in WLS program. We aimed to compare the longitudinal agreement of MRI-M and MRI-C for assessing PDFF change. Our study found that while MRI-M underestimates PDFF values compared with MRI-C cross-sectionally, the bias is constant and small and as a result, the two techniques agree closely in estimating rate of PDFF change during both rapid (visits 1 to 3) and slow (visits 3 to 5) PDFF reduction periods. We observed a bias of − 0.13% per month (MRI-M–MRI-C) in the rate of PDFF change for visits 1 to 3, and a bias of 0.03% per month (MRI-M–MRI-C) in the rate of PDFF change for visits 3 to 5 ($p > 0.05$). These biases were not statistically significant and were so small that they are not likely to be of clinical importance. Our results suggest that either technique of PDFF estimation (MRI-M or MRI-C) could be used by individual sites for purposes of multi-center studies evaluating PDFF change as an endpoint. However, the consistent difference in PDFF measured by both techniques over time reinforces the idea that the same technique should be used for longitudinal follow-up. Thus, while either technique may be suitable for use by a particular site for a clinical trial or by a particular imaging center for clinical care, the two techniques should not be used interchangeably in the same patient.

Previous studies have demonstrated the accuracy and precision of both MRI-M and MRI-C techniques for PDFF estimation with respect to reference-standard MRS, cross-sectionally and longitudinally [4, 8–10, 36, 38]. Similar to the results from prior studies [11, 23, 26], we found that MRI-M PDFF estimations are ~ 0.6% lower than MRI-C PDFF estimations across the full range of PDFF values seen clinically. The source of underestimation can be ascribed to both acquisition and analysis. In acquisition, if T2* component is ignored (as it is the same for both MRI-M and MRI-C), for the typical sequence parameters used by MRI-M and MRI-C in this study, both techniques slightly overestimate PDFF with MRI-C overestimating slightly more than MRI-M. For analysis, as discussed in Haufe et al [23, 26], the magnitude fitting used by MRI-M has a Rician noise distribution, which adds an extra signal to the liver at all echo times, reducing the relative signal oscillation and causing PDFF underestimation. Our results add to the body of existing literature by demonstrating that this small bias between techniques is relatively constant at each time point allowing for very similar estimations of PDFF reduction. Moreover, in the authors' experience, MRI-M and MRI-C PDFF maps do not differ substantially in image quality, even in the low PDFF range, suggesting that errors caused by Rician noise distribution for MRI-M reconstruction do not meaningfully reduce the signal to noise ratio or impair the quality of the corresponding PDFF maps.

Our study has several limitations. Our analysis was limited by the relatively small sample size overall ($n = 54$), the even smaller sample size of patients completing all five visits ($n = 29$), the exclusive focus on adult NAFLD, and the use of MRI systems from one manufacturer, primarily at one field strength. Validation studies are needed to further

compare these techniques across a wider range of participants, potentially including obese children with NAFLD and/or adults with steatosis due to conditions other than NAFLD, with different drug interventions and using scanners by different manufacturers and of different field strengths. Additionally, almost all changes in PDFF in our analysis were unidirectional, which was not unexpected given that WLS is efficacious for the reduction of liver fat content [30, 39]. Nonetheless, future studies may focus on ensuring that the techniques agree for PDFF increase as well as reduction over time. Finally, although we confirmed a small bias in PDFF estimated by MRI-M and MRI-C, our study was not designed to determine which technique is more accurate relative to a ground truth.

In conclusion, while there is a small difference between MRI-M and MRI-C techniques, the rates of PDFF change estimated by MRI-M and MRI-C agree closely. These findings support the use of either technique by individual sites for future multi-center studies that include PDFF change as an endpoint, pending further validation in larger multi-center studies. The option to use either technique will increase the flexibility of site selection for such trials. However, our study results also emphasize that while either technique may be suitable for use by a particular site for a clinical trial or by a particular imaging center for clinical care, the two techniques should not be used interchangeably in the same patient.

Supplementary Material

Refer to Web version on PubMed Central for supplementary material.

Funding information

This study has received funding by R01 DK088925.

Abbreviations

CSE-MRI	Chemical-shift-encoded MRI
ICC	Intraclass correlation coefficient
MRI-C	Magnetic resonance imaging—complex-based
MRI-M	Magnetic resonance imaging—magnitude-based
MRS	Magnetic resonance spectroscopy
NAFLD	Nonalcoholic fatty liver disease
PDFF	Proton density fat fraction
ROI	Region of interest
VLCD	Very low–calorie diet
WLS	Weight loss surgery

References

1. Reeder SB, Hu HH, Sirlin CB (2012) Proton density fat-fraction: a standardized MR based biomarker of tissue fat concentration. J Magn Reson Imaging 36:1011–1014 [PubMed: 22777847]
2. Reeder SB, Sirlin CB (2010) Quantification of liver fat with magnetic resonance imaging. Magn Reson Imaging Clin N Am 18:337– 357 [PubMed: 21094444]
3. Hernando D, Liang ZP, Kellman P (2010) Chemical shift-based water/fat separation: a comparison of signal models. Magn Reson Med 64:811–822 [PubMed: 20593375]
4. Zand KA, Shah A, Heba E et al. (2015) Accuracy of multiecho magnitude-based MRI [M-MRI] for estimation of hepatic proton density fat fraction [PDFF] in children. J Magn Reson Imaging 42: 1223–1232 [PubMed: 25847512]
5. Kuhn JP, Hernando D, Mensel B et al. (2014) Quantitative chemical shift- encoded MRI is an accurate method to quantify hepatic steatosis. J Magn Reson Imaging 39:1494–1501 [PubMed: 24123655]
6. Bashir MR, Zhong X, Nickel MD et al. (2015) Quantification of hepatic steatosis with a multistep adaptive fitting MRI approach: prospective validation against MR spectroscopy. AJR Am J Roentgenol 204:297–306 [PubMed: 25615751]
7. Zhong X, Nickel MD, Kannengiesser SA, Dale BM, Kiefer B, Bashir MR (2014) Liver fat quantification using a multi-step adaptive fitting approach with multi-echo GRE imaging. Magn Reson Med 72:1353–1365 [PubMed: 24323332]
8. Yu H, Shimakawa A, Hines CD et al. (2011) Combination of complex-based and magnitude-based multiecho water-fat separation for accurate quantification of fat-fraction. Magn Reson Med 66:199–206 [PubMed: 21695724]
9. Johnson BL, Schroeder ME, Wolfson T et al. (2014) Effect of flip angle on the accuracy and repeatability of hepatic proton density fat fraction estimation by complex data-based, T1-independent, T2*-corrected, spectrum-modeled MRI. J Magn Reson Imaging 39: 440–447 [PubMed: 23596052]
10. Hines CD, Frydrychowicz A, Hamilton G et al. (2011) T[1] independent, T[2][*] corrected chemical shift based fat-water separation with multi-peak fat spectral modeling is an accurate and precise estimate of hepatic steatosis. J Magn Reson Imaging 33:873–881 [PubMed: 21448952]
11. Tyagi A, Yeganeh O, Levin Y et al. (2015) Intra- and inter-examination repeatability of magnetic resonance spectroscopy, magnitude-based MRI, and complex-based MRI for estimation of hepatic proton density fat fraction in overweight and obese children and adults. Abdom Imaging 40:3070–3077 [PubMed: 26350282]
12. Xu L, Duanmu Y, Blake GM, Zhang C et al. (2018) Validation of goose liver fat measurement by QCT and CSE-MRI with biochemical extraction and pathology as reference. Eur Radiol 28: 2003–2012 [PubMed: 29238866]
13. Hoy AM, McDonald N, Lennen RJ et al. (2018) Non-invasive assessment of liver disease in rats using multiparametric magnetic resonance imaging: a feasibility study. Biol Open 7 10.1242/bio.033910
14. Bannas P, Kramer H, Hernando D et al. (2015) Quantitative magnetic resonance imaging of hepatic steatosis: validation in ex vivo human livers. Hepatology 62:1444–1455 [PubMed: 26224591]
15. Permutt Z, Le TA, Peterson MR et al. (2012) Correlation between liver histology and novel magnetic resonance imaging in adult patients with non-alcoholic fatty liver disease - MRI accurately quantifies hepatic steatosis in NAFLD. Aliment Pharmacol Ther 36:22– 29 [PubMed: 22554256]
16. Tang A, Desai A, Hamilton G et al. (2015) Accuracy of MR imaging-estimated proton density fat fraction for classification of dichotomized histologic steatosis grades in nonalcoholic fatty liver disease. Radiology 274:416–425 [PubMed: 25247408]
17. Kuhn JP, Hernando D, Munoz del Rio A et al. (2012) Effect of multipeak spectral modeling of fat for liver iron and fat quantification: correlation of biopsy with MR imaging results. Radiology 265:133–142 [PubMed: 22923718]
18. Middleton MS, Heba ER, Hooker CA et al. (2017) Agreement between magnetic resonance imaging proton density fat fraction measurements and pathologist-assigned steatosis grades of

liver biopsies from adults with nonalcoholic steatohepatitis. Gastroenterology 153:753–761 [PubMed: 28624576]

19. Middleton MS, Van Natta ML, Heba ER et al. (2018) Diagnostic accuracy of magnetic resonance imaging hepatic proton density fat fraction in pediatric nonalcoholic fatty liver disease. Hepatology 67: 858–872 [PubMed: 29028128]
20. Loomba R, Sirlin CB, Ang B et al. (2015) Ezetimibe for the treatment of nonalcoholic steatohepatitis: assessment by novel magnetic resonance imaging and magnetic resonance elastography in a randomized trial [MOZART trial]. Hepatology 61:1239–1250 [PubMed: 25482832]
21. Le TA, Chen J, Changchien C et al. (2012) Effect of colesevelam on liver fat quantified by magnetic resonance in nonalcoholic steatohepatitis: a randomized controlled trial. Hepatology 56:922– 932 [PubMed: 22431131]
22. Noureddin M, Lam J, Peterson MR et al. (2013) Utility of magnetic resonance imaging versus histology for quantifying changes in liver fat in nonalcoholic fatty liver disease trials. Hepatology 58:1930– 1940 [PubMed: 23696515]
23. Loomba R, Sanyal AJ (2013) The global NAFLD epidemic. Nat Rev Gastroenterol Hepatol 10:686–690 [PubMed: 24042449]
24. Cui J, Philo L, Nyugen P et al. (2016) Sitagliptin vs. placebo for non-alcoholic fatty liver disease: a randomized controlled trial. J Hepatol 65:369–376 [PubMed: 27151177]
25. Ajmera VH, Cachey E, Ramers C et al. (2019) MRI assessment of treatment response in HIV-associated NAFLD: a randomized trial of a Stearoyl-coenzyme-A-desaturase-1 inhibitor (ARRIVE trial). Hepatology 70:1531–1545 [PubMed: 31013363]
26. Haufe WM, Wolfson T, Hooker CA et al. (2017) Accuracy of PDFF estimation by magnitude-based and complex-based MRI in children with MR spectroscopy as a reference. J Magn Reson Imaging 46:1641–1647 [PubMed: 28323377]
27. https://www.cdc.gov/obesity/adult/defining.html. Accessed on 5 Dec 2018
28. Fazeli SD, Fowler KJ, Mamidipalli A et al. (2019) Hepatic steatosis and reduction in steatosis following bariatric weight loss surgery differs between segments and lobes. Eur Radiol 29:2474–2480 [PubMed: 30547206]
29. Pooler BD, Wiens CN, MsMillan A et al. (2019) Monitoring fatty liver disease with MRI following bariatric surgery: a prospective dual-center study. Radiology 290:682–690 [PubMed: 30561273]
30. Yokoo T, Serai SD, Pirasteh A, Bashir MR, Hamilton G, Hernando D, Hu HH, Hetterich H, Kühn JP, Kukuk GM, Loomba R, Middleton MS, Obuchowski NA, Song JS, Tang A, Wu X, Reeder SB, Sirlin CB, Proton Density Fat Fraction Committee RSNAQIBA (2018) Linearity, bias, and precision of hepatic proton density fat fraction measurements by using MR imaging: a meta-analysis. Radiology 286:486–498 [PubMed: 28892458]
31. Yokoo T, Shiehmorteza M, Hamilton G et al. (2011) Estimation of hepatic proton- density fat fraction by using MR imaging at 3.0 T. Radiology 258:749–759 [PubMed: 21212366]
32. Yokoo T, Bydder M, Hamilton G et al. (2009) Nonalcoholic fatty liver disease: diagnostic and fat-grading accuracy of low-flip-angle multiecho gradient- recalled-echo MR imaging at 1.5 T. Radiology 251:67–76 [PubMed: 19221054]
33. Kuhn JP, Jahn C, Hernando D et al. (2014) T1 bias in chemical shift-encoded liver fat-fraction: role of the flip angle. J Magn Reson Imaging 40:875–883 [PubMed: 24243439]
34. Liu CY, McKenzie CA, Yu H, Brittain JH, Reeder SB (2007) Fat quantification with IDEAL gradient echo imaging: correction of bias from T1 and noise. Magn Reson Med 58:354–364 [PubMed: 17654578]
35. Bydder M, Yokoo T, Hamilton G et al. (2008) Relaxation effects in the quantification of fat using gradient echo imaging. Magn Reson Imaging 26:347–359 [PubMed: 18093781]
36. Reeder SB, McKenzie CA, Pineda AR et al. (2007) Water-fat separation with IDEAL gradient-echo imaging. J Magn Reson Imaging 25:644–652 [PubMed: 17326087]
37. Hamilton G, Yokoo T, Bydder M et al. (2011) In vivo characterization of the liver fat [1]H MR spectrum. NMR Biomed 24:784–790 [PubMed: 21834002]
38. Tang A, Tan J, Sun M et al. (2013) Nonalcoholic fatty liver disease: MR imaging of liver proton density fat fraction to assess hepatic steatosis. Radiology 267:422–431 [PubMed: 23382291]

39. Patel NS, Doycheva I, Peterson MR et al. (2015) Effect of weight loss on MRI estimation of liver fat and volume in patients with nonalcoholic steatohepatitis. Clin Gastroenterol Hepatol 13:561–565 [PubMed: 25218667]

40. Yu H, Shimakawa A, McKenzie CA, Brodsky E, Brittain JH, Reeder SB (2008) Multiecho water-fat separation and simultaneous R2* estimation with multifrequency fat spectrum modeling. Magn Reson Med 60:1122–1134 [PubMed: 18956464]

Key Points

- MRI-M demonstrates a significant but small and consistent bias (0.5–0.7%; $p < 0.001$) towards underestimation of PDFF compared with MRI-C at 3 T.
- Rates of PDFF change estimated by MRI-M and MRI-C agree closely (ICC 0.96–0.98) in adults with severe obesity and biopsy-proven NAFLD enrolled in a weight loss surgery program.
- Our findings support the use of either MRI technique (MRI-M or MRI-C) for clinical care or by individual sites or for multi-center trials that include PDFF change as an endpoint. However, since there is a bias in their measurements, the same technique should be used in any given patient for longitudinal follow-up.

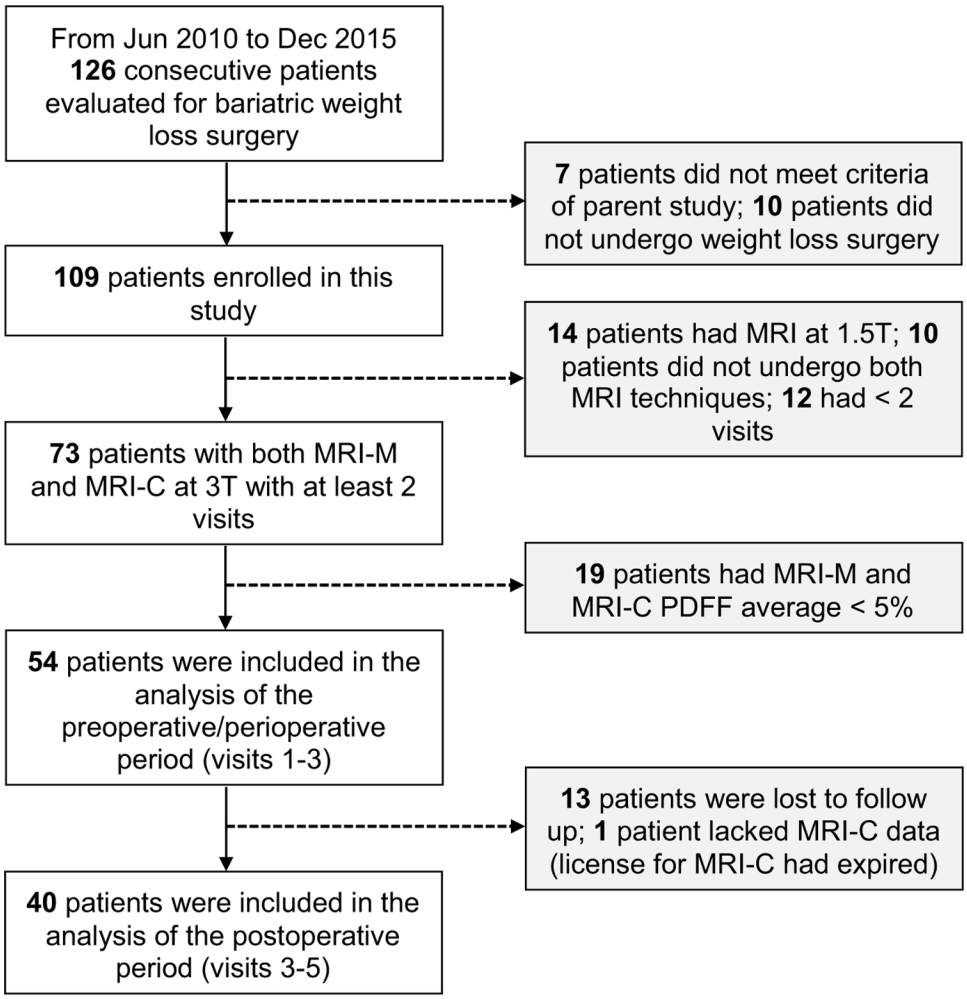

Fig. 1.

Flow chart of study cohort. MRI-M, MRI-C magnitude-based, and complex-based MRI; PDFF proton density fat fraction

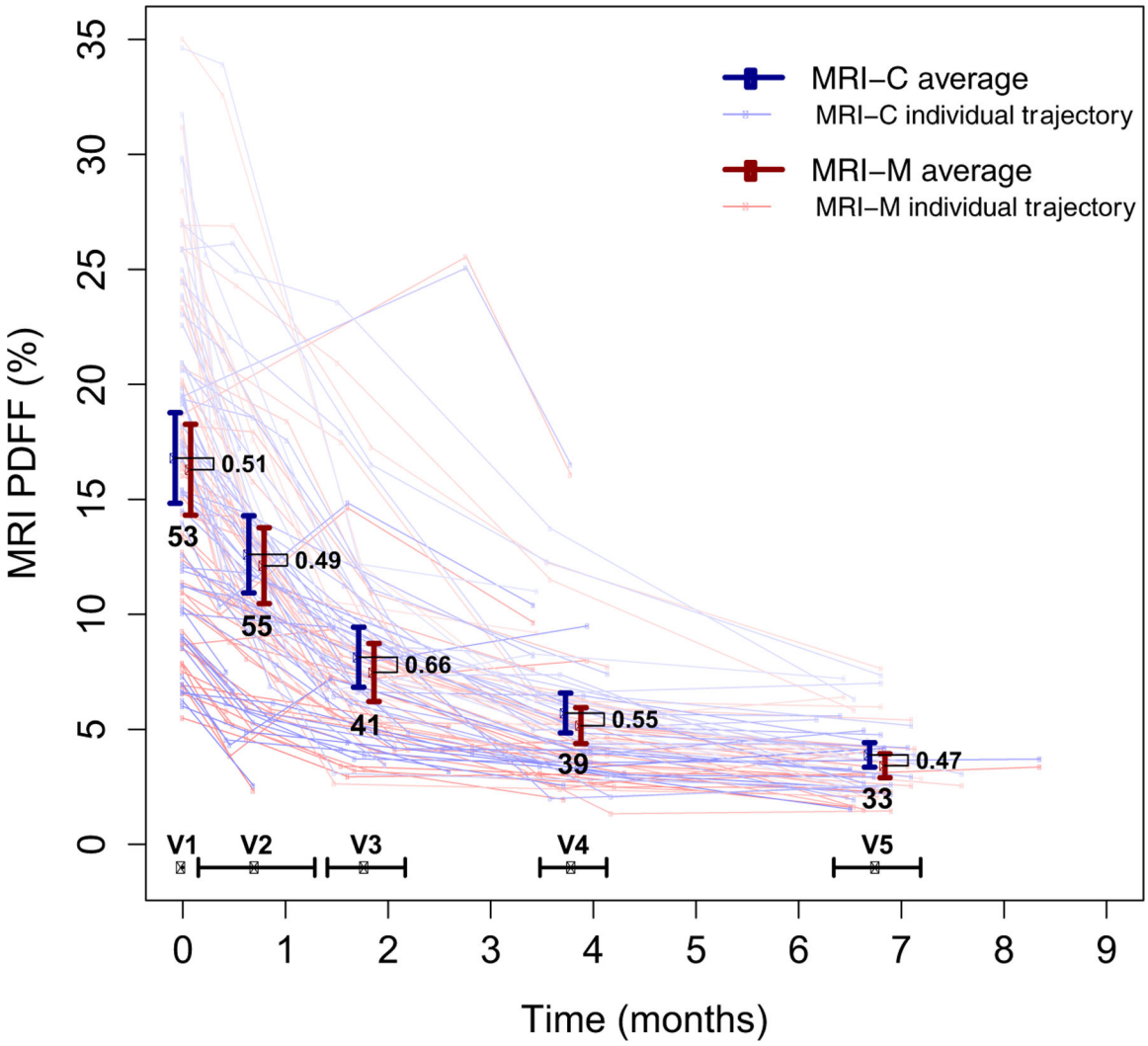

Fig. 2.

PDFF decline over time. Shown here are mean PDFF values over the course of the five study visits showing that rates of PDFF change are similar for the MRI-C (blue) and the MRI-M (red) techniques. The PDFF change pattern was biphasic for both techniques; more rapid linear decline was seen from visits 1 to 3, and then slower linear decline was seen from visits 3 to 5. The bars around the PDFF means and visit means are 95% confidence intervals (CIs) and standard deviations (SDs), respectively. The number of patients for each visit and the mean differences in PDFF between MRI-C and MRIM are overlain. The overall *p* value for the mean differences for all visits is < 0.001

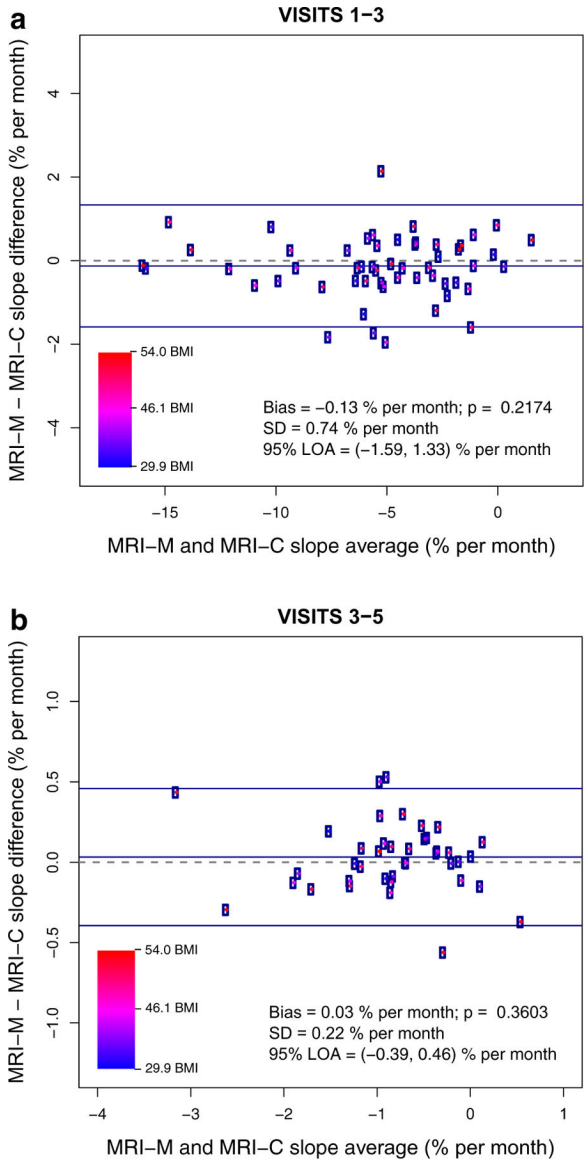

Fig. 3.

PDFF change with MRI-M and MRI-C for visits 1 to 3, and visits 3 to 5 color coded by baseline BMI. Bland-Altman plot for visits 1 to 3 (**a** with $n = 54$ patients), and visits 3 to 5 (**b** with $n = 40$ patients), illustrating the difference between rate of hepatic PDFF change estimated by MRI-M and MRI-C as a function of average rate of PDFF change. Bias (the middle blue line, which is the mean of MRI-M and MRI-C differences) and its p value, standard deviation (SD) of the MRI-M and MRI-C differences, limits of agreement (LOA), and range of baseline BMI values are overlain

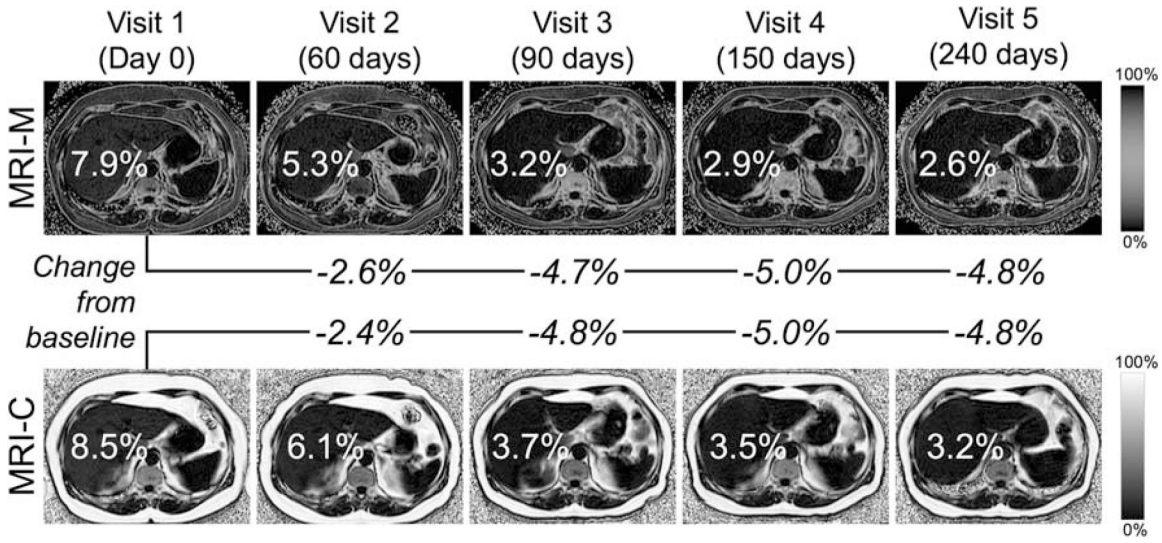

Fig. 4.

Change in PDFF from baseline with MRI-M and MRI-C. Both CSE-MRI techniques (magnitude and complex) agree in estimating PDFF change in a 52-year-old woman. MRI-M- and MRI-C-estimated PDFF values are overlain on PDFF maps. Changes in PDFF from baseline are shown between the two rows of images. The dynamic scales for the parametric PDFF maps are 0–50% for MRI-M and 0– 100% for MRI-C

Table 1

Parameters for MRI techniques

Technique	MRI-M	MRI-C
Pulse sequence	2D SGRE	3D SGRE
Slice thickness (mm)	8	8
Flip angle (degrees)	10	3
Interslice gap (mm)	0	Not applicable
TE (ms)	1.15, 2.3,3.45, 4.6,5.75,6.9	0.9, 1.7, 2.5, 3.2, 4.0, 4.7
TR (ms)	≥ 150	6.9
Base image matrix	224 × 128	192×160
FOV (mm)	440 ×440	440 × 440
NEX	1	1
Type of parallel imaging	ASSET	ARC
R	1.25	2×2
Bandwidth (± kHz)	±142	±125
Acquisition time (s)	2 × 20[a]	20

MRI-M and *MRI-C* magnitude-based and complex-based magnetic resonance imaging, *SGRE* spoiled gradient recalled echo, *TE* time to echo, *TR* repetition time, *FOV* field of view, *NEX* number of excitations, *R* acceleration factor, *ASSET* assay spatial sensitivity encoding technique, *ARC* auto-calibrating reconstruction for cartesian sampling

[a]Two 20-s breatholds required to cover the whole liver

Table 2

Cohort characteristics (baseline and on final visit)

Sex	*n*	Age in years Mean ± SD (range)	BMI on 1st visit in kg/m^2 Mean ± SD (range)	BMI on final visit in kg/m^2 Mean ± SD (range)	MRI-M PDFF on 1st visit in percent Mean ± SD (range)	MRI-M PDFF on final visit in percent Mean ± SD (range)	MRI-C PDFF on 1st visit in percent Mean ± SD (range)	MRI-C PDFF on final visit in percent Mean ± SD (range)
All	54	52 ± 12 (27–70)	42.3 ± 5.0 (30.0–54.0)	34.3 ±4.7 (25.048.1)	16.1 ±7.2 (5.5–35)	5.1 ±3.7 (1.5–17.7)	16.6 ±7.2 (6.0–34.6)	5.6 ±3.7 (1.5–17.2)
Males	10	54 ±11 (31–69)	41.8 ±4.3 (33.7–16.2)	35.3 ±3.1 (28.5–10.2)	17.9±5.6 (7.1–27.1)	7.3 ±5.4 (1.6–17.7)	19.1 ±5.7 (9.0–30.1)	7.8 ±5.2 (1.9–17.2)
Females	44	52 ± 11.8 (27–70)	42.7 ±5.0 (30.0–54.0)	34.1 ±5.0 (25XM8.1)	15.6 ±7.5 (5.5–35.0)	4.7 ± 3.1 (1.5–16.1)	16.2 ±7.4 (6.0–34.6)	5.0 ± 3.1 (1.5–15.1)

PDFF proton density fat fraction, *BMI* body mass index, *SD* standard deviation

Table 3

Per-visit summary of differences in PDFF between MRI-M and MRI-C

Visit	N	Months (mean ± SD)	MRI-C PDFF (mean ± SD)	MRI-M PDFF (mean ± SD)	MRI-C (−) MRI-M PDFF (mean ± SD)	*p* value
1	53	0	16.8 ±7.3	16.3 ± 7.3	0.5 ± 1.0	0.00027
2	55	0.7 ±0.6	12.6 ± 6.4	12.1 ± 6.3	0.5 ± 0.9	0.00025
3	41	1.8 ±0.4	8.2 ± 4.3	7.5 ± 4.1	0.7 ± 0.7	0.00002
4	39	3.8 ±0.3	5.7 ± 2.8	5.2 ± 2.5	0.5 ± 0.8	0.00015
5	33	6.8 ±0.4	3.9 ± 1.6	3.4 ± 1.5	0.5 ± 0.5	0.00002

SD standard deviation